Journal of Neuroscience Research

Journal of Neuroscience Research 88:3243–3256 (2010)

Axon Growth and Guidance Genes Identify Nascent, Immature, and Mature Olfactory Sensory Neurons

Jeremy C. McIntyre, William B. Titlow, and Timothy S. McClintock*

Department of Physiology, University of Kentucky, Lexington, Kentucky

Neurogenesis of projection neurons requires that axons be initiated, extended, and connected. Differences in the expression of axon growth and guidance genes must drive these events, but comprehensively characterizing these differences in a single neuronal type has not been accomplished. Guided by a catalog of gene expression in olfactory sensory neurons (OSNs), in situ hybridization and immunohistochemistry revealed that *Cxcr4* and *Dbn1*, two axon initiation genes, marked the developmental transition from basal progenitor cells to immature OSNs in the olfactory epithelium. The CXCR4 immunoreactivity of these nascent OSNs overlapped partially with markers of proliferation of basal progenitor cells and partially with immunoreactivity for GAP43, the canonical marker of immature OSNs. Intracellular guidance cue signaling transcripts *Ablim1, Crmp1, Dypsl2, Dpysl3, Dpysl5, Gap43, Marcskl1,* and *Stmn1–4* were specific to, or much more abundant in, the immature OSN layer. Receptors that mediate axonal inhibition or repulsion tended to be expressed in both immature and mature OSNs (*Plxna1, Plxna4, Nrp2, Efna5*) or specifically in mature OSNs (*Plxna3, Unc5b, Efna3, Epha5, Epha7*), although some were specific to immature OSNs (*Plxnb1, Plxnb2, Plxdc2, Nrp1*). Cell adhesion molecules were expressed either by both immature and mature OSNs (*Dscam, Ncam1, Ncam2, Nrxn1*) or solely by immature OSNs (*Chl1, Nfasc1, Dscaml1*). Given the loss of intracellular signaling protein expression, the continued expression of guidance cue receptors in mature OSNs is consistent with a change in the role of these receptors, perhaps to sending signals back to the cell body and nucleus.

Key words: axonogenesis; cell adhesion; neurogenesis; growth cone; neural development

The major task of neural development is to generate the synaptic circuits that provide the basis for the complex functions of the nervous system. Most neurons extend axons that grow to appropriate targets via recognition of positive and negative cues in the surrounding environment (Tessier-Lavigne and Goodman, 1996). As a neuron matures, the shift from axon elongation to axon homeostasis is reflected by changes in gene expression (Skene and Willard, 1981a,b; Li et al., 1995; Smith and Skene, 1997; Blackmore and Letourneau, 2006). Expression of genes associated with axon outgrowth decreases while expression of genes involved in growth inhibition increases. To assess the changes in guidance cue signaling between immature and mature neurons, we compared the expression of a large number of axonal growth and guidance genes in olfactory sensory neurons (OSNs). Because of the continuous turnover of OSNs, immature and mature OSNs coexist at all ages. They can be distinguished by their differential expression of several genes, but the definitive marker genes are *Gap43* for immature OSNs and *Omp* for mature OSNs.

The synaptic partners of OSNs are the dendrites of projection neurons and interneurons in the glomeruli of the olfactory bulb (Pinching and Powell, 1971; Royet et al., 1988). Glomeruli have specific identities and locations, defined by the innervation of each glomerulus solely by the axons of OSNs expressing the same odorant receptor, but the mechanisms involved are not fully understood (Ressler et al., 1994; Vassar et al., 1994; Mombaerts et al., 1996; Strotmann et al., 2000; Schaefer et al., 2001; Kobayakawa et al., 2007; Soucy et al., 2009). Studies of mice with targeted deletions of single classical guidance cues or cell adhesion molecules have not revealed major defects in glomerular formation or location (Treloar et al., 1997; Cloutier et al., 2002, 2004; Montag-Sallaz et al., 2002; Schwarting et al., 2000, 2004; Walz et al., 2002, 2006; Cutforth et al., 2003; Cho et al., 2007; Hasegawa et al., 2008; Kaneko-

J.C. McIntyre's current address is Department of Pharmacology, University of Michigan, 1150 W. Medical Center Drive, Ann Arbor, MI 48109-5632.

Contract grant sponsor: National Institutes of Health; Contract grant number: R01 DC007194 (to T.S.M.).

*Correspondence to: Timothy S. McClintock, Department of Physiology, University of Kentucky, 800 Rose St., Lexington, KY 40536-0298. E-mail: mcclint@uky.edu

Received 27 October 2009; Revised 13 June 2010; Accepted 22 July 2010

Published online 29 September 2010 in Wiley Online Library (wileyonlinelibrary.com). DOI: 10.1002/jnr.22497

Goto et al., 2008). These experiments suggest that classical guidance cues may be important for guiding axons to regions of the bulb and restricting axon growth to the glomerular layer but do not yet show that these cues determine the fine-scale positioning of glomeruli.

Odorant receptor-mediated signaling and neuronal activity are alternative mechanisms for determining glomerular location. Odorant receptor identity itself is a crucial component of axon convergence into glomeruli and the precise location of glomeruli (Mombaerts et al., 1996; Feinstein and Mombaerts; 2004; Feinstein et al., 2004). Glomerular position and homogeneity of glomerular innervation appear to depend on cAMP levels and the activation of GNAS ($G_{\alpha s}$) and ADCY3 (AC3) located in OSN axons (Belluscio et al., 1998; Lin et al., 2000; Zheng et al., 2000; Yu et al., 2004; Imai et al., 2006; Chesler et al., 2007; Col et al., 2007; Zou et al., 2007). Another possible mechanism is odorant receptor-mediated cAMP regulation of expression of some axon guidance and cell adhesion molecule genes (Imai et al., 2006, 2008; Serizawa et al., 2006; Kaneko-Goto et al., 2008).

The diversity and complexity of potential mechanisms regulating the growth of OSN axons argues for a more complete understanding of axon growth and guidance genes expressed by immature and mature OSNs. Recent evidence indicates that OSNs express several hundred genes related to axon growth and guidance (Sammeta et al., 2007). We hypothesized that many of these genes are differentially expressed between immature and mature OSNs. Distinguishing the axon guidance capabilities of immature and mature OSNs will help in identifying mechanisms of OSN axon growth and maintenance. Herein we demonstrate differences in the abundance of axon growth and guidance mRNAs between immature and mature OSNs, including the discovery that nascent OSNs can be identified by expression of two axon initiation genes, *Cxcr4* and *Dbn1*.

MATERIALS AND METHODS

In Situ Hybridization and Immunofluorescence

Male C57Bl/6J mice, aged postnatal day 21–25 (P21–P25), were used unless indicated otherwise. In situ hybridization was performed as described previously (Shetty et al., 2005; Yu et al., 2005). A detailed protocol is available from the authors. Briefly, mice were anesthetized via intraperitoneal injection with ketamine hydrochloride (10 mg/ml) and xylazine (1 mg/ml) in 0.9% saline (0.01 ml/g body weight) and transcardially perfused with 4% paraformaldehyde. The maxillary and anterior cranial region of the head (snout) was dissected free and fixed in 4% paraformaldehyde overnight, followed by decalcification in EDTA overnight, and cryoprotected in sucrose, embedded in OCT, and stored at −80°C. Coronal sections 10 μm thick were cut on a cryostat and mounted on Superfrost Plus slides (Fisher Scientific, Pittsburgh, PA). Digoxygenin-labeled riboprobes were prepared from cDNA fragments ranging from 400 bp to 1,000 bp in size. Most mRNAs were detected with a single riboprobe; however, to increase signal strength, two riboprobes were pooled to detect some mRNAs. Sense controls were invariably negative.

For immunofluorescence, 10-μm cryosections were prepared using the same methods as for in situ hybridization, except that fixation was for 1.5 hr in 4% paraformaldehyde. Slides were washed three times for 10 min each in 1× PBS and permeabilized for 30 min in 1% Triton X-100 in 1× PBS at room temperature, followed by blocking at room temperature for 30 min with 5% normal donkey serum, 0.4% Triton X-100, in 1× PBS (blocking buffer). Slides were incubated overnight at 4°C in primary antibodies diluted in blocking buffer. Slides were then washed twice with 0.05% Tween 20, 1× PBS and incubated at room temperature in appropriate secondary antibody for 1 hr. The following primary antibodies were used: goat anti-CXCR4 (1:250; Capralogics; CI0116, amino acids 14–40 of mouse CXCR4), rabbit anti-GAP43 (1:200; Millipore, Bedford, MA; AB5220), mouse anti-NCAM1 (1:1,000; Sigma-Aldrich, St. Louis, MO; C9672), rabbit antiphospho-histone H3 (1:200; Millipore; 06-570), and mouse anti-Ki67 (1:50; Vector Laboratories, Burlingame, CA; VP-K452, clone MM1). Secondary antibodies, all used at a dilution of 1:500, were Dylight549 donkey anti-goat, Dylight488 donkey anti-rabbit, Dylight 488 donkey anti-mouse from Jackson Immunoresearch (West Grove, PA). The use and specificity of phospho-histone H3, GAP43, Mki67, and NCAM1 antibodies have previously been demonstrated (Kee et al., 2002; Zimmer et al., 2004; Akins and Greer, 2006; Dudanova et al., 2007). The CXCR4 antibody has also been used previously (Nishiumi et al. 2005), and immunostaining replicates *Cxcr4* expression detected by in situ hybridization. To increase the frequency of detection of proliferating basal cells, immunohistochemistry for phosphohistone H3 and Mki67 was done with sections prepared from young mice (age P4).

Digital images were acquired with either a Spot 2e camera (Diagnostics Instruments, Sterling Heights, MI) mounted on a Nikon Diaphot 300 inverted microscope or a Spot 2e camera on a Nikon Eclipse Ti-U inverted microscope. Processing of images to adjust size, brightness, and contrast was done in Adobe Photoshop, and organization of figures was done in Deneba Canvas.

Counts of labeled cells were done on three tissue sections per mouse (age P21–P25) to generate an average count for each mouse. Labeled cells in coronal sections were visually identified and manually counted at two positions along the olfactory epithelium (the dorsal recess and the septum) per section. Cell counts were normalized to the total length of epithelium used for counting. To correct for overcounting, Abercrombie's formula was used with a measured nuclear diameter of 3.1 ± 0.4 μm to obtain a correction factor of 0.76 (Abercrombie, 1946). Student's *t*-tests at $\alpha = 0.05$ were used to assess statistical significance.

Olfactory Bulbectomy

All procedures using mice were approved by an Institutional Animal Care and Use Committee and conformed to NIH guidelines. Adult male C57BL/6 mice (6 weeks) were

anesthetized with ketamine/xylazine as described above. A midline sagittal incision was made in the scalp to expose the cranium, and a 2-mm hole over one bulb was drilled into the skull using a diamond-tipped burr. Eight mice were subjected to unilateral bulbectomy by aspiration. Gelfoam soaked in sterile saline was used to fill the cavity, and the skin was sutured with 6-0 Ethilon suture. Recovery from surgery was aided by warming, subcutaneous injection of 0.5 ml saline, and maintenance on buprenorphine for 48 hr. Food and water were supplied ad libitum.

RNA Isolation and Quantitative RT-PCR

Eight mice were euthanized 7 days after bulbectomy. The septal epithelium and olfactory turbinates were dissected into 700 μl of ice-cold TriReagent (Molecular Research Center, Cincinnati, OH) and homogenized using a polytron. RNA was then extracted using the Tri Reagent protocol supplied by the manufacturer. The yield and quality of RNA samples were determined with a UV-spectrophotometer and a model 2100 Bioanalyzer (Agilent Technologies, Palo Alto, CA).

Primers with melting temperatures between 58°C and 60°C were designed using Primer Express software (Applied Biosystems, Foster City, CA) and purchased from Integrated DNA Technologies (Coralville, IA). Complementary DNA was prepared by reverse transcription of 0.5 μg total RNA using Superscript II reverse transcriptase and random hexamers (Invitrogen, Carlsbad, CA) in 50-μl reactions. Amplification of samples was performed in triplicate using an ABI 7700 Sequence Detection System. Samples were run using Sybr Green 2× Master mix (Applied Biosystems, Foster City, CA). Thermal cycler conditions were 95°C for 15 min, then 45 cycles of 95°C for 15 sec, 60°C for 1 min. Melt curve analysis was used to confirm that only a single product was generated in each reaction. The mean of each triplicate set was calculated, and these data were normalized using the geometric mean of four control mRNAs in each tissue sample; *Actb* (actin, beta), *Hprt1* (hypoxanthine guanine phosphoribosyl transferase 1), *GAPDH* (glyceraldehyde-3-phosphate dehydrogenase), and *Ubc* (ubiquitin C). Ipsilateral samples from bulbectomized mice were compared against contralateral samples using one-tailed paired *t*-tests. Correction for multiple testing was done using Holm's stepwise correction method (Holm, 1979).

RESULTS

Most Axon Guidance Genes Are Developmentally Regulated

We hypothesized that immature and mature OSNs differ in expression of axon growth and guidance genes because the needs of their axons differ. Directed by data from expression profiling studies of the olfactory epithelium or of purified samples of OSNs (Shetty et al., 2005; Sammeta et al., 2007), we selected 36 genes that encode proteins involved in axon growth and guidance and tested their expression patterns in the olfactory epithelium. Twenty-two mRNAs were differentially abundant between immature and mature OSNs. Seventeen mRNAs were detected primarily in immature OSNs, five mRNAs only in mature OSNs, another 13 mRNAs in both immature and mature OSNs, and one mRNA in the lamina propria (Table I). All but two, *Ncam2* and *Nrp2*, were expressed uniformly across the odorant receptor expression zones of the olfactory epithelium, indicating that few genes correlate with this zonal organization and its effects on axonal connections to the olfactory bulb. The restriction of *Ncam2* and *Nrp2* to the ventral olfactory epithelium had previously been established (Yoshihara et al., 1997; Norlin et al., 2001).

Maturation Changes Guidance Cue Local Signaling

The mRNAs whose expression was detected primarily in immature OSNs encode guidance cue receptors and intracellular signaling molecules (Fig. 1). In fact, among the mRNAs that encode intracellular signaling proteins that control the behavior and extension of growth cones, all were detected in immature OSNs and weakly, if at all, in mature OSNs. *Ppp2cb*, the catalytic subunit of protein phosphatase 2A, a protein important for promoting neuritogenesis, was expressed by immature OSNs (Fig. 1B). Transcripts for *Marcskl1*, encoding a protein similar in function to GAP43, were similarly enriched in immature OSNs (Fig. 1C). *Ablim1*, which mediates the attractive effects of netrin, was specific to immature OSNs (Fig. 1D; Lundquist et al., 1998). The related mRNA, *Ablim2*, was detected at similar intensities in both mature and immature OSNs (Fig. 1E). Although ABLIM2 has been shown to bind F-actin, (Barrientos et al., 2007) whether ABLIM2 is a mediator of signals that control growth cone behavior is as yet untested. Three members of the dihydropyrimidinase-like family; *Crmp1, Dpysl3,* and *Dpysl5*, which encode dihydropyrimidinase-like proteins (also known as collapsin-response mediator proteins) that mediate growth cone collapse and turning in response to semaphorins were detected only in immature OSNs (Fig. 1F–H). Another member of this family, *Dpysl2*, was detected strongly in immature OSNs and weakly in mature OSNs (Fig. 1I). We also tested the expression of four stathmin genes whose encoded proteins interact with the microtubule network to regulate axon extension and turning (Sobel, 1991; Ozon et al., 1997; Grenningloh et al., 2003). *Stmn1* and *Stmn2* were expressed exclusively in immature OSNs, as previously shown (Camoletto et al., 2001; Pellier-Monnin et al., 2001), consistent with their roles in promoting axonal growth for other types of neurons (Morii et al., 2006; Fig. 1J,K). *Stmn3* and *Stmn4* were expressed in both immature and mature OSNs (Fig. 1L,M). STMN3 and STMN4 act to reduce axon branching, a property consistent with expression that spans the differentiation boundary into mature OSNs, which have relatively few branches (Baldassa et al., 2007; Cao et al., 2007; Poulain and Sobel, 2007). Taken together, these findings indicate reduced local signaling by guidance cue receptors in mature OSNs, suggesting a

TABLE I. Summary of Genes Tested[†]

Gene symbol	OMP+/– ratio	OBX microarray	Cell type by ISH	Gene name	Entrez gene ID
Ablim1	0.20	1.6★	iOSN	Actin-binding LIM protein 1	226251
Ablim2	1.50	nd	OSN	Actin-binding LIM protein 2	231148
Chl1	0.50	3.1★	iOSN	Cell adhesion molecule with homology to L1cam	12661
Crmp1	1.10	1	iOSN	Collapsin response mediator protein 1	12933
Cxcl12	0.30	1.2	lamina propria (age P0)	Chemokine (C-X-C motif) ligand 12	20315
Cxcr4	0.04	2.1★	iOSN, basal	Chemokine (C-X-C motif) receptor 4	12767
Dbn1	0.50	2.6★	iOSN, basal	Drebrin 1	56320
Dpysl2	0.90	0.8	OSN	Dihydropyrimidinase-like 2	12934
Dpysl3	0.30	1.5★	iOSN	Dihydropyrimidinase-like 3	22240
Dpysl5	0.80	nd	iOSN	Dihydropyrimidinase-like 5	65254
Dscam	2.00	nd	OSN	Down's syndrome cell adhesion molecule	13508
Dscaml1	0.80	1.7	iOSN	Down's syndrome cell adhesion molecule-like 1	114873
Efna3	5.60	0.5★	mOSN	Ephrin A3	13638
Efna5	1.70	nd	OSN	Ephrin A5	13640
Epha5	50.80	0.4	mOSN	Eph receptor A5	13839
Epha7	2.50	0.6★	mOSN	Eph receptor A7	13841
Gap43	0.60	1.5★	iOSN	Growth-associated protein 43	14432
Marcksl1	0.30	1.4★	iOSN	MARCKS-like 1	17357
Ncam1	1.70	0.8★	OSN	Neural cell adhesion molecule 1	17967
Ncam2	2.90	0.7★	OSN	Neural cell adhesion molecule 2	17968
Nfasc	0.90	nd	iOSN	Neurofascin	269116
Nrp1	1.10	1	OSN	Neuropilin 1	18186
Nrp2	0.70	nd	OSN	Neuropilin 2	18187
Nrxn1	1.60	nd	OSN	Neurexin I	18189
OMP	44.40	0.3★	mOSN	Olfactory marker protein	18378
Plxdc2	0.50	nd	iOSN	Plexin domain containing 2	67448
Plxna1	1.80	nd	OSN	Plexin A1	18844
Plxna3	7.60	0.4★	mOSN	Plexin A3	18846
Plxna4	4.10	nd	OSN	Plexin A4	243743
Plxnb1	0.90	nd	iOSN	Plexin B1	235611
Plxnb2	0.90	1	iOSN	Plexin B2	140570
Ppp2cb	0.50	1.2★	iOSN	ser/thr Protein phosphatase 2a, catalytic subunit, beta isoform	19053
Robo2	1.30	nd	OSN	Roundabout homolog 2 (*Drosophila*)	268902
Stmn1	0.70	1.5★	iOSN	Stathmin 1	16765
Stmn2	0.7	1.2★	iOSN	Stathmin-like 2	20257
Stmn3	1.90	1	OSN	Stathmin-like 3	20262
Stmn4	6.30	0.7★	OSN	Stathmin-like 4	56471
Unc5b	3.50	nd	mOSN	unc-5 Homolog B	107449

[†]OMP+/– ratio column specifies the degree of enrichment in mature OSNs (Sammeta et al., 2007). OBX (olfactory bulbectomy) microarray column shows -fold changes in mRNA abundance for olfactory epithelium samples at 7 days after OBX (Shetty et al., 2005). OSN, both immature and mature OSNs; iOSN, immature OSNs; mOSN, mature OSNs; nd, not detected or not present on the microarray.
★Significant difference between sham and bulbectomized mice, $P < 0.05$.

maturational shift in the type of signaling mediated by guidance cue receptors in OSN axons.

Immature OSNs Express a Unique Set of Guidance Receptors and Cell Adhesion Molecules

Several guidance cue receptors and a cell adhesion molecule were detected only in immature OSNs. The semaphorin receptors *Plxnb1* and *Plxnb2* and the plexin domain containing receptor *Plxdc2* were detected in immature OSNs (Fig. 2A–C). Another semaphorin receptor, *Nrp1*, gave a mosaic pattern among immature OSNs (Fig. 2D). This mosaicism is likely determined by odorant receptor signaling (Imai et al., 2006; 2008). We also detected three cell adhesion molecules, *Chl1*, *Nfasc1*, and *Dscaml1*, only in immature OSNs (Fig. 2E–G). Overall, these findings indicate that immature OSNs detect guidance cue signals different from those detected by mature OSNs.

Axon Initiation Genes Mark the Transition From Basal Cell to Immature OSN

Two mRNAs shared a novel expression pattern. *Dbn1* and *Cxcr4* mRNAs were detected toward the basal side of the epithelium in a thin band of cells that did not match the locations of basal cells or immature OSNs (Fig. 3). Basal cells are proliferative progenitors that give rise to the OSNs, and, as shown in Figure 1A, they occupy mostly the first two cell diameters apical to the

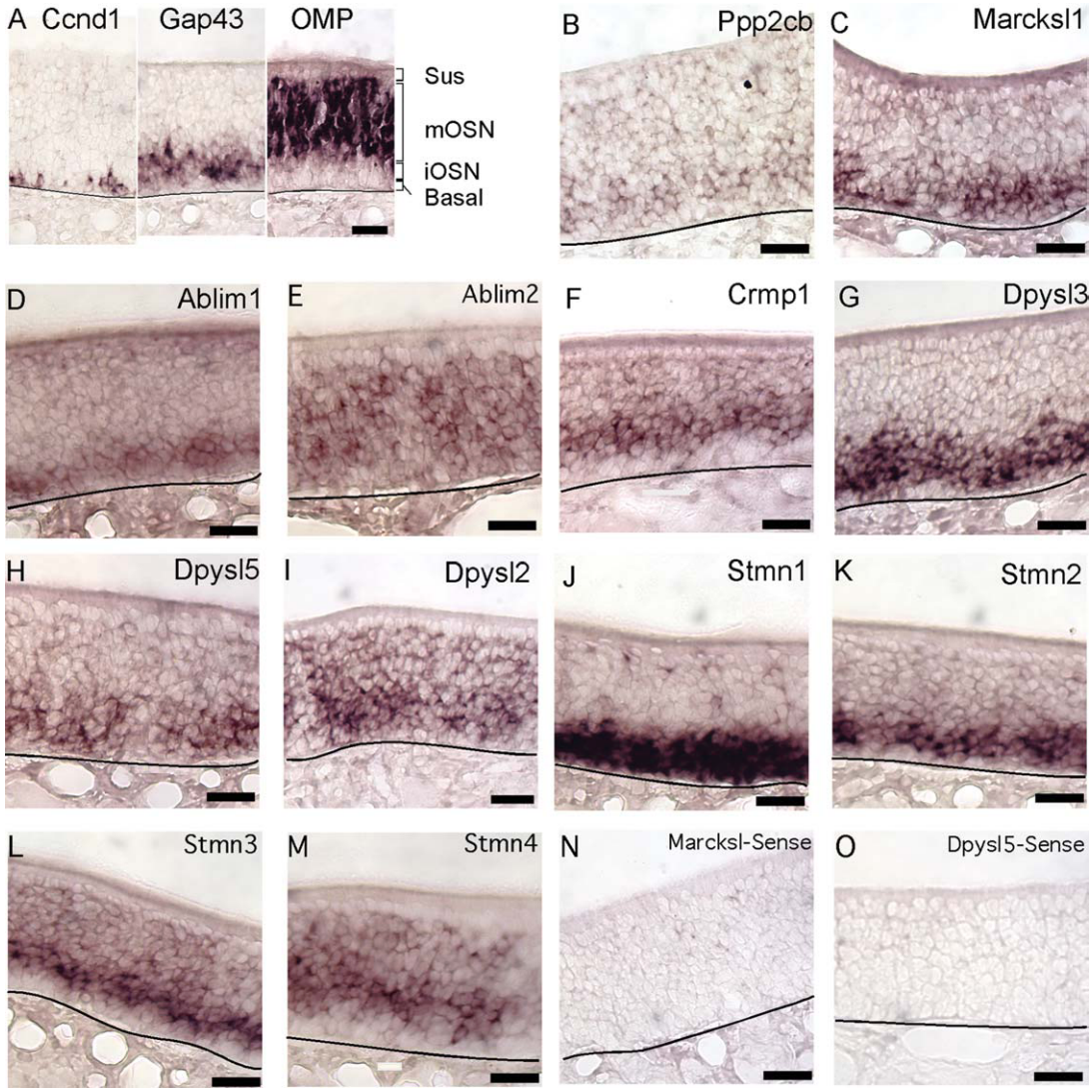

Fig. 1. Messenger RNAs encoding proteins that regulate growth cone dynamics were expressed primarily in immature OSNs. **A:** Guide to the cell body layers of the olfactory epithelium. *Ccnd1* labels a subset of basal cells; *Gap43* labels immature OSNs; *OMP* labels mature OSNs. Sus, unlabeled sustentacular cell body layer; mOSN, mature OSN cell body layer; iOSN, immature OSN cell body layer; basal, basal cell layer. **B–D:** *Ppp2cb, Marcksl1,* and *Ablim1* were detected in immature OSNs. **E:** *Ablim2* was detected in immature and mature OSNs. **F–H:** *Crmp1, Dpysl3,* and *Dpysl5* were detected in immature OSNs. **I:** *Dpysl2* was detected in immature and mature OSNs. **J,K:** *Stmn1* and *Stmn2* were detected in immature OSNs. **L,M:** *Stmn3* and *Stmn4* were detected in immature and mature OSNs. **N,O:** Examples of the absence of labeling when sense probes were used. Lines, location of basal lamina. Scale bars = 20 μm. [Color figure can be viewed in the online issue, which is available at wileyonlinelibrary.com.]

basal lamina of the olfactory epithelium. Lying apical to the basal cells are immature OSNs (Figs. 1A, 3A,C) produced by the basal cells. The distinctive patterns of *Dbn1* and *Cxcr4* expression suggested that these cells might mark the transition from basal cell to immature OSNs. Several pieces of evidence were consistent with this hypothesis. First, transitional cells should be located adjacent to basal cells. Cells expressing *Dbn1* and *Cxcr4* transcripts were located at two to three cell diameters above the basal lamina at positions where markers of either basal cells or immature OSNs can also be detected (Figs. 1A, 3A–D). Second, as a transitional cell type, nascent OSNs should be less numerous than immature OSNs. Alternate sections detected thinner regions of labeling for *Dbn1* and *Cxcr4* than for *Gap43*, the canonical marker of immature OSNs (Fig. 3A–D). Third, these transitional cells should be at least as common as the cells that give rise to OSNs, the *Neurog1*-positive basal cell. Cells expressing *Cxcr4* and *Dbn1* transcripts formed a more continuous layer than *Neurog1*-positive basal cells, which occur in clusters in age P21 mice from our colony, suggesting that *Cxcr4*- and *Dbn1*-positive cells are

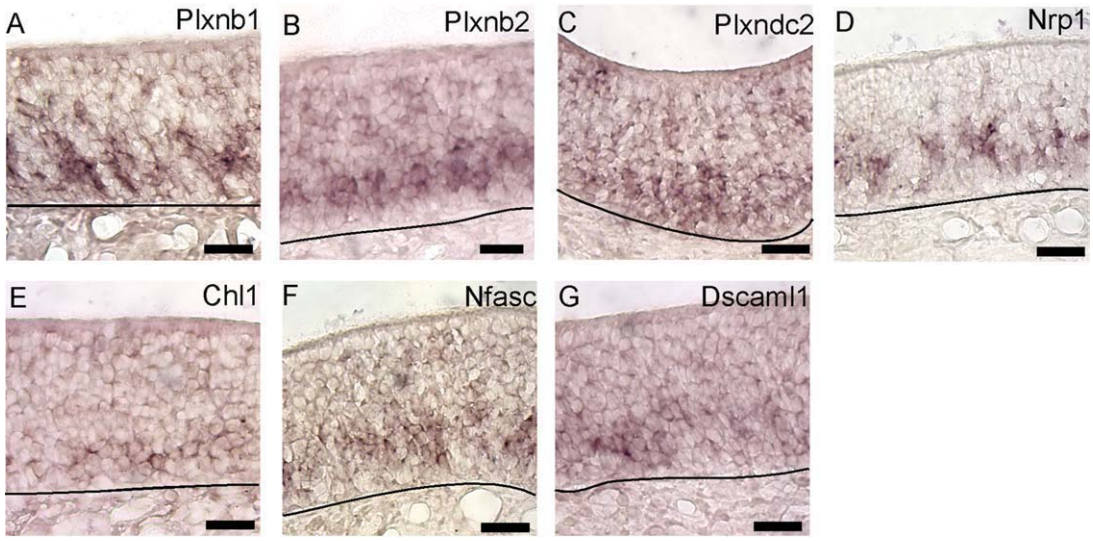

Fig. 2. **A–G:** Guidance cue receptor and cell adhesion molecule mRNAs expressed primarily by immature OSNs. **A–G:** Images of in situ hybridization for *Plxnb1, Plxnb2, Plxdc2, Nrp1, Chl1, Nfasc,* and *Dscaml1*. Lines, location of basal lamina. Scale bars = 20 μm. [Color figure can be viewed in the online issue, which is available at wileyonlinelibrary.com.]

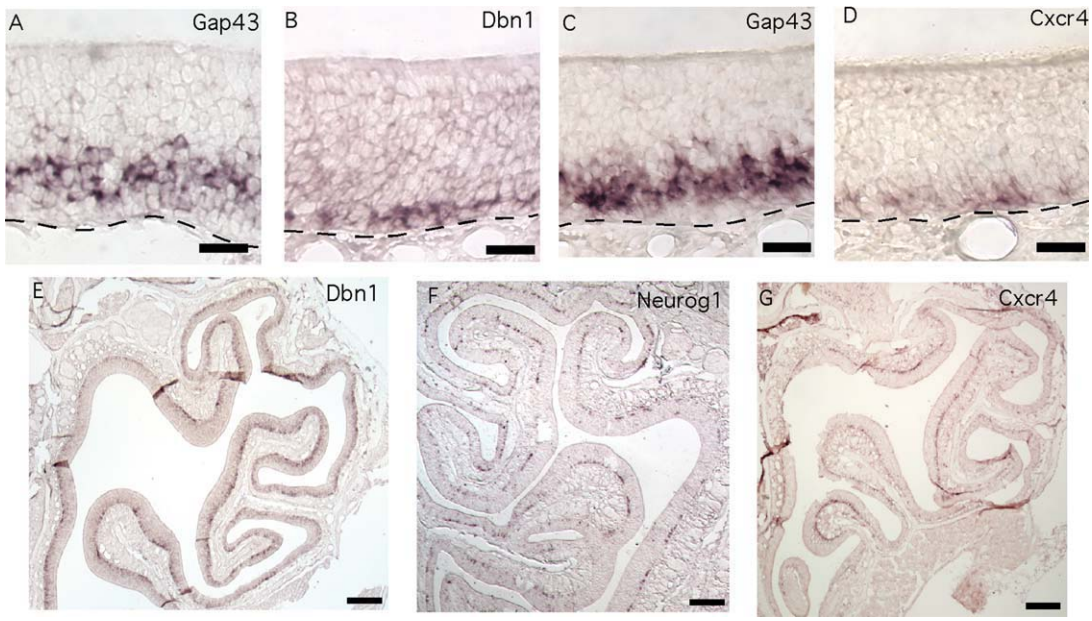

Fig. 3. Basally located cells express axon initiation mRNAs. **A–D:** *Dbn1* (B) and *Cxcr4* (D) mRNAs were expressed in a thin layer of cells that may partially overlaps with the basal end of the immature OSN layer marked by adjacent sections hybridized for *Gap43* mRNA (A,C). **E–G:** Cells expressing *Dbn1* (E) and *Cxcr4* (G) formed a nearly continuous layer throughout the olfactory epithelium, compared with the clusters of cells positive for *Neurog1* (F), the canonical marker of immediate neuronal precursors. Lines, location of basal lamina. Scale bars = 20 μm in A–D; 100 μm in E–G. [Color figure can be viewed in the online issue, which is available at wileyonlinelibrary.com.]

more numerous (Fig. 3E–G). Indeed, cells expressing *Cxcr4* were more abundant than *Neurog1*-positive cells (9.0 ± 0.8 per 0.1 mm, n = 3 mice vs. 2.8 ± 0.5 per 0.1 mm, n = 3 mice), indicating that cells expressing *Cxcr4* could not consist solely of the immediate neuronal precursor type of globose basal cell. Fourth, transitional cells should rapidly differentiate into the well-known population of immature OSNs, so they are likely to overlap somewhat with markers of immature OSNs. Cells immunoreactive for both CXCR4 and GAP43 were rare (0.8 ± 0.5 per 0.1 mm, n = 3 mice) but identifiable, indicating that these two populations par-

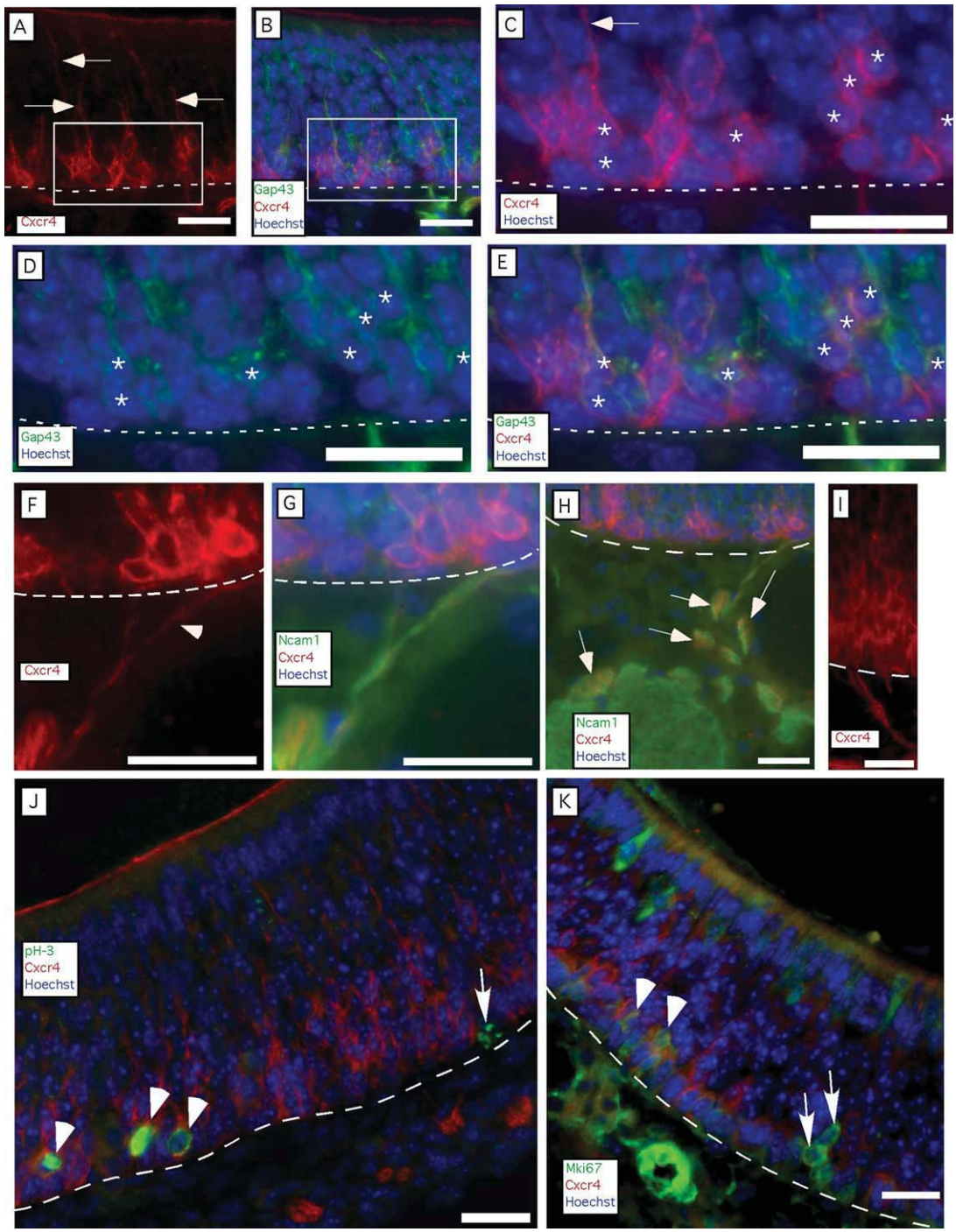

Fig. 4. CXCR4 immunoreactivity identifies cells located two to four cell diameters apical to the basal lamina. **A–E:** CXCR4-immunoreactive processes extended toward the apical surface of the olfactory epithelium (arrows), and some cells are immunoreactive for both CXCR4 and GAP43. C–E: A region where cells immunoreactive for both CXCR4 and GAP43 (asterisks) were abundant. The arrow indicates an apical process labeled by CXCR4 immunoreactivity. **F,G:** Basal processes immunoreactive for CXCR4 (arrowhead in F) crossed the basal lamina and entered olfactory nerve bundles, where they were associated with NCAM1-positive axons. **H:** Broader view of the integration of CXCR4-immunoreactive fibers (some identified by arrows) into the bundles of NCAM1-immunoreactive fascicles of the olfactory nerve. **I:** Example of CXCR4-immunoreactive fibers exiting the base of the olfactory epithelium. **J,K:** In P4 mice, in which the frequency of proliferating basal cells is higher than in older mice, some proliferating basal cells marked by phosphorylated histone H3 (pH-3) or by Mki67 were also marked by CXCR4 immunoreactivity (arrowheads), but others were not (arrows). Lines, location of basal lamina. Scale bars = 20 μm. [Color figure can be viewed in the online issue, which is available at wileyonlinelibrary.com.]

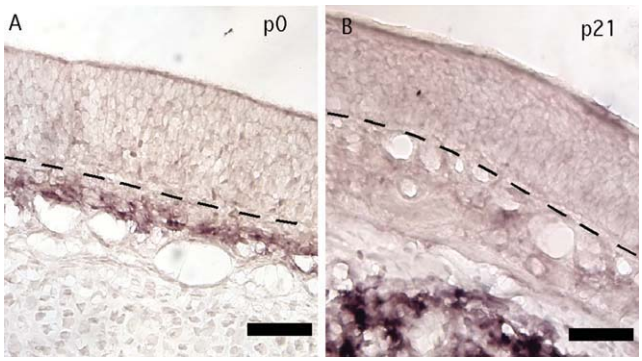

Fig. 5. *Cxcl12* was expressed beneath the olfactory epithelium in an age-dependent pattern. **A:** *Cxcl12* was expressed in the lamina propria at age P0. **B:** At age P21, *Cxcl12* was instead detected in cells within the bone underlying the lamina propria. Images from the nasal septum are shown. Lines, location of basal lamina. Scale bars = 20 μm. [Color figure can be viewed in the online issue, which is available at wileyonlinelibrary.com.]

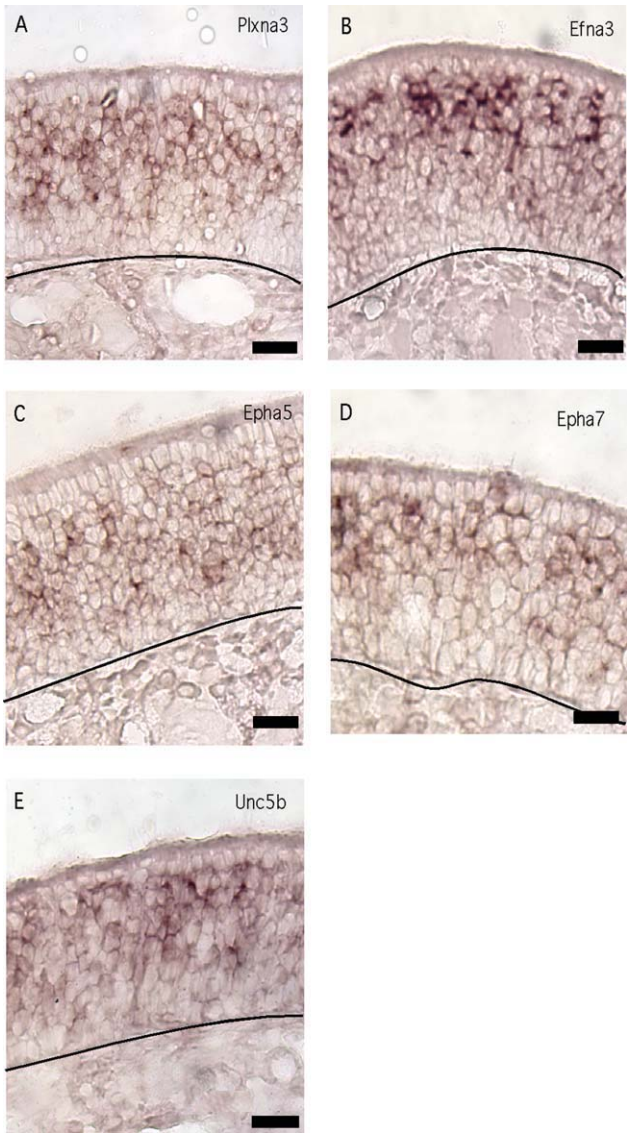

Fig. 6. Guidance cue receptor mRNAs expressed primarily in mature OSNs. **A–E:** *Efna3, Epha5, Epha7, Plxna3,* and *Unc5b* displayed this pattern of expression. Lines, location of basal lamina. Scale bars = 20 μm. [Color figure can be viewed in the online issue, which is available at wileyonlinelibrary.com.]

tially overlap (Fig. 4A–E). Fifth, if the transitional cells become neurons, they might have neurites, an apical dendritic process, and a basal axon. Many CXCR4-immunoreactive cells had apical and basal processes (Fig. 4A–I). Nerve fascicles containing CXCR4-immunoreactive neurites could be seen exiting the base of the olfactory epithelium and joining olfactory nerve bundles along with NCAM1 positive axons, evidence that these processes were axons (Fig. 4F–I). In addition, these CXCR4-immunoreactive fibers were detected in only a fraction of the area of olfactory nerve bundles identified by NCAM1 immunoreactivity (Fig. 4H). This is consistent with the relative abundance of mature OSNs and immature OSNs compared with CXCR4-immunoreactive cells in the olfactory epithelium. We did not detect CXCR4 immunoreactivity in the olfactory nerve layer of the olfactory bulb. Sixth, if CXCR4-immunoreactive cells are indeed transitional, some of them should also show overlap with immunoreactivity for markers specific to basal cells. To test this hypothesis, we used young mice (age P4) because the frequency of proliferating basal cells is high in neonates. We observed numerous instances of CXCR4 immunoreactivity in cells that were also immunoreactive for phosphorylated histone-3, a marker of active mitosis (Fig. 4J). We also observed overlap with MKI67 immunoreactivity, another marker of basal cell proliferation (Fig. 4K). These findings are consistent with the hypothesis that *Cxcr4* and *Dbn1* are expressed by cells in transition from globose basal cells to immature OSNs.

Expression of *Cxcr4* by cells in the olfactory epithelium led us to search for cells expressing the CXCR4 agonist CXCL12. *Cxcl12* was expressed nearby in a developmentally regulated pattern. At age P21 (Fig. 5C,D), *Cxcl12* mRNA was detected deep in the bone and cartilage below the lamina propria, but, at P0, *Cxcl12* was detected in cells of the lamina propria directly below the basal lamina of the olfactory epithelium (Fig. 5A,B), the direction taken by OSN axons.

Cell Adhesion Molecules and Receptors for Inhibitory Signals Predominate in Mature Neurons

Mature OSNs expressed several guidance cue receptors that were not detected in immature OSNs. *Plxna3*, a receptor for the secreted semaphorin 3, was expressed only by mature OSNs (Fig. 5A). Of the ephrins and eph receptors we tested, *Efna3, Epha5,* and *Epha7*, were detected primarily in mature OSNs (Fig. 6B–D). Finally, *Unc5b*, which mediates inhibitory effects of netrin, was expressed by mature OSNs (Fig. 6E).

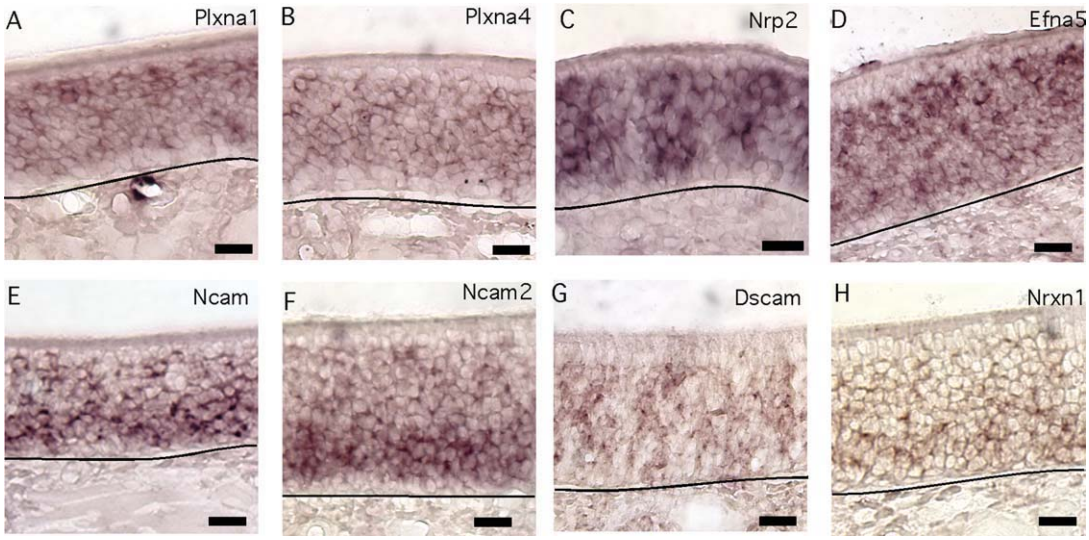

Fig. 7. Guidance cue receptor and cell adhesion molecule mRNAs detected in both immature and mature OSNs. **A–H:** *Plxna1, Plxna4, Efna5, Nrp2, Nrxn1,* and *Ncam1* displayed this pattern. Lines, location of basal lamina. Scale bars = 20 μm. [Color figure can be viewed in the online issue, which is available at wileyonlinelibrary.com.]

Seven receptor mRNAs were detected at approximately equal levels in immature and mature OSNs. The semaphorin receptors *Plxna1* and *Plxna4* were expressed in both cell types, with *Plxna1* exhibiting a punctate staining pattern and *Plxna4* showing more uniform expression (Fig. 7A,B). The semaphorin receptor *Nrp2* was detected in both immature and mature OSNs (Fig. 7C) and, as shown previously, was limited to the ventral region of the olfactory epithelium (Norlin et al., 2001). *Efna5* was also expressed in both immature and mature OSNs (Fig. 7D). The cell adhesion molecules *Ncam1, Ncam2, Dscam,* and *Nrxn1* were detected in both cell types (Fig. 7E–H), and, though clearly detectable in mature OSNs, *Ncam1* and *Nrxn1* gave slightly stronger labeling in the immature OSN layer. As shown previously, *Ncam2* expression was restricted to the ventral olfactory epithelium (Yoshihara et al., 1997).

Immature OSN mRNAs Increase After Bulbectomy

The interpretations of the expression patterns that we observed depend on correct identification of mature and immature OSNs. To confirm our cell type identification, we used olfactory bulbectomy, which results in the death of mature OSNs and an increase in the production of immature OSNs in a relatively synchronous wave that appears to peak at about 7 days after bulbectomy (Schwob, 2002; Shetty et al., 2005). Transcripts judged by anatomical position as enriched in immature OSNs should be more abundant in the olfactory epithelium following bulbectomy, and, conversely, mature OSN-enriched transcripts should decrease. We performed unilateral bulbectomy on 6-week-old C57Bl/6 mice and measured changes in mRNA abundance by quantitative RT-PCR for 10 mRNAs. As expected, *Omp* abundance was fivefold less in olfactory epithelium ipsilateral to the ablated olfactory bulb compared with contralateral olfactory epithelium ($t = -7.73$, $n = 6$ mice, $P < 0.0005$). *Cbr2* was used as a negative control because it is specific to sustentacular cells, which are unaffected by bulbectomy (Monti Graziadei and Graziadei 1979; Costanzo, 1985; Yu et al., 2005). As expected, *Cbr2* mRNA abundance was unaltered ($t = 1.57$, $n = 6$ mice, $P > 0.1$). In contrast, *Ablim1, Marcksl1, Plxnb1,* and *Dpysl3* gave statistically significant increases (Table II).

Among the 15 mRNAs that had in situ hybridization patterns indicative of expression primarily in immature OSNs (Figs. 1, 2), none decrease after bulbectomy but eight are now known to increase in abundance 5–7 days after bulbectomy (Tables I, II). Among the six mRNAs that had in situ hybridization patterns indicative of expression primarily in mature OSNs (Figs. 1A, 6), none increase after bulbectomy, but four are known to decrease (Table I). Physical mapping by in situ hybridization correctly distinguishes mRNAs expressed primarily by immature and mature OSNs. As long as expression is consistent within these layers and not restricted to a small minority of cells (as might happen with infiltrating macrophages, for example), this approach is valid.

DISCUSSION

Using OSNs as a source of tissue where mature and immature neurons always coexist, we found maturational differences in gene expression. Cells expressing *Dbn1* and *Cxcr4*, two axon initiation genes, had a unique expression pattern. Immunoreactivity for CXCR4 revealed labeling of a population of transitional cells that overlapped basally with markers of proliferating basal cells and apically with a marker of immature

TABLE II. Bulbectomy Increases Immature OSN Transcripts[†]

Gene name	Gene symbol	Fold change	*t*-Statistic	*P* value
Plexin B1	*Plxnb1*	1.57	9.4943	0.0005★
Olfactory maker protein	*OMP*	0.19	–7.7311	0.0005★
MARCKS-like protein	*Marcksl1*	2.49	5.5804	0.0025★
Actin-binding LIM protein 1	*Ablim1*	2.52	4.7242	0.005★
Dihydropyrimidinase-like 3	*Dpysl3*	2.94	4.3564	0.005★
Chemokine (C-X-C motif) receptor 4	*Cxcr4*	2.95	3.8308	0.01
Growth-associated protein 43	*Gap43*	2.58	3.2391	0.025
Plexin B2	*Plxnb2*	1.43	2.7576	0.025
Drebrin 1	*Dbn1*	1.77	2.6478	0.025
Carbonyl reductase 2	*Cbr2*	1.29	1.5793	0.1

[†]Real-time quantitative RT-PCR results comparing olfactory epithelia ipsilateral and contralateral to unilateral olfactory bulbectomy at 7 days postlesion. Correction for multiple testing adjusted the α level to <0.01.
★Significant difference between sham and bulbectomized mice, $P < 0.05$.

OSNs. Many of these transitional cells displayed the beginnings of a neuronal morphology, arguing that these cells are nascent OSNs. Immature OSNs express a larger variety of mRNAs for intracellular axon guidance signaling proteins than do mature OSNs. While mature OSNs express few intracellular axon guidance signaling genes, they do express guidance cue receptors and cell adhesion molecules in numbers similar to those of immature OSNs, and many of these are shared between the two developmental stages. The expression patterns that we observed indicate that OSN axon growth to the olfactory bulb occurs in several phases and indicate certain proteins in each phase.

Maturation Is Marked by Changes in the Axon Guidance Signaling Network

As expected, the majority of mRNAs encoding axon guidance-related intracellular signaling proteins were detected only in immature OSNs. Among 14 tested, we detected only three such mRNAs, *Dpysl2, Stmn3,* and *Stmn4*, in both immature and mature OSNs, and even these were more abundant in immature OSNs. Reduced expression of these genes coincides with the loss of the growth cone and the need to regulate its cytoskeletal dynamics. We detected in immature OSNs the expression of nine mRNAs for proteins that are known to regulate actin and microtubule dynamics in response to guidance cue receptor activation. Immature OSNs likely have broad signaling networks to allow integration of multiple attractive and repulsive cues. In contrast, mature OSNs express many fewer mRNAs encoding intracellular signaling proteins.

The receptors detected specifically in mature OSNs typically mediate repulsive or inhibitory effects. Guidance cue receptors in mature OSNs could help to maintain the position of the axon and its terminals, but expression of most of the downstream signaling molecules that link these receptors to the cytoskeletal dynamics of the axon was either absent or decreased. We therefore suspect that guidance cue receptors perform as yet undiscovered functions in mature OSNs that differ from their axon guidance role in immature OSNs. Recent evidence from other types of neurons indicates that some guidance cue receptors can generate signals that regulate transcription (Bong et al., 2007; Rhee et al., 2007), suggesting that the retention of guidance cue receptors in mature OSNs corresponds with a change from local control in the growth cone to sending homeostatic signals back to the cell body and nucleus.

Phenotypically Distinct Stages of OSN Axon Growth

OSNs are the only type of neuron in which the cell body exists in the periphery and extends an axon to a synaptic target in the brain. Our data support the interpretation that OSN axon growth consists of several phenotypically distinct stages. First, newly born immature OSNs must initiate an axon and extend it through the basal lamina into the lamina propria. We found that a population of basally located cells specifically expresses two genes, *Dbn1* and *Cxcr4*, known to be involved in axon initiation and extension (Shirao et al., 1992; Ishikawa et al., 1994; Toda et al., 1999; Chalasani et al., 2003, 2007; Lieberam et al., 2005; Miyasaka et al., 2007; Geraldo et al., 2008). The expression of *Cxcr4* overlapped partially with expression of the immature OSN marker *Gap43* and partially with markers of basal cell proliferation, indicating that expression of *Cxcr4* identifies cells in transition from a basal cell to an OSN phenotype. Together, the number of immediate neuronal precursor subtype of globose basal cells expressing *Neurog1* and the degree of overlap in expression of *Gap43* and *Cxcr4* could account for about half of the cells expressing *Cxcr4*. Therefore, some cells that express *Cxcr4* are probably a unique transitional phenotype not identified by the canonical markers for immature OSNs or the immediate neuronal precursor type of globose basal cell. These transitional cells appear quickly to acquire a neuronal phenotype, because many CXCR4-immunoreactive cells showed evidence of neurites, including labeling in fascicles of axons in the lamina propria. We refer to these cells as nascent OSNs.

We hypothesize that DBN1 and CXCR4 contribute to the initiation of the axon and promote its exten-

sion through the basal lamina and out of the olfactory epithelium. CXCR4 is a G-protein-coupled receptor that inhibits adenylyl cyclase in some cell types but appears primarily to stimulate cAMP and its downstream signaling pathways in neurons (Chalasani et al., 2003). In differentiating neurons, the neurite that produces more cAMP is the neurite that forms the axon (Shelly et al., 2010). The presence of CXCR4 in nascent OSNs and the location of its agonist, CXCL12, in the underlying lamina propria in newborn mice may therefore provide a signal ensuring that the basal neurite of the new OSN forms the axon. The positive effect of CXCR4/CXCL12 signaling on axonal extension (Toba et al., 2008) is therefore oriented to promote the extension of nascent OSN axons out of the olfactory epithelium. In the new OSN axon, activated CXCR4 may also contribute to robust axonal extension via the ability of cAMP to spur axonal growth and suppress or reverse the effects of inhibitory guidance cues (Song et al., 1997; Cai et al., 1999). Indeed, the growth of OSN axons out of explants of embryonic olfactory epithelium is reduced in the absence of CXCR4 or in the presence of a CXCR4 antagonist (Toba et al., 2008).

Once they have left the olfactory epithelium proper, OSN axons turn toward the olfactory bulb. The cue, or cues, responsible for this turn of the pioneering axons is unknown, although the migratory mass that accompanies these axons may help provide it (Doucette, 1989, 1990). Netrin and CXCL12 may attract axons toward the bulb, insofar as they both are expressed in the mesenchyme surrounding the olfactory epithelium and are enriched near the cribriform plate. Immature OSNs should respond to netrin as they express not only DCC but also DSCAM, which can act as a netrin receptor (Ly et al., 2008). The lamina propria provides a favorable axon growth environment, in that it contains laminin, fibronectin, and collagen-IV (Gong and Shipley, 1996; Whitesides and LaMantia, 1996) as well as boundaries created by the expression of chondroitin sulfate proteoglycans (CSPG), thereby establishing what should be permissive paths for axons to pass through the cribriform plate to the olfactory bulb (Shay et al., 2008).

Immature OSN axons must navigate across the surface of the olfactory bulb in the outer olfactory nerve layer until they reach the appropriate domain, where they then defasciculate, enter the inner olfactory nerve layer, refasciculate, and coalesce into glomeruli (Au et al., 2002). Guidance cue receptors expressed in immature OSNs are probably important for targeting the correct domains. The olfactory bulb expresses multiple cues that appear to establish subdomains, such as *Sema3a, Sema3f, Slit-1,* and *Netrin-4* (Cloutier et al., 2002; Cho et al., 2007; Williams et al., 2007). We detected strong expression of receptors for these molecules in immature OSNs. Immature OSNs detect SEMA3A via NRP1 and several plexin receptors, signaling events that may help to keep immature axons in the outer olfactory nerve layer. An example of guidance cue signaling changes that accompany the transition from immaturity to maturity is netrin signaling. The netrin receptors *Dcc* and *Dscam* that mediate axon attraction were detected in immature OSNs, along with *Ablim1*, an important downstream signaling molecule linked to *Dcc* (Astic et al., 2002; Gitai et al., 2003; Ly et al., 2008; Andrews et al., 2008). Mature OSNs, however, express *Unc5b*, a receptor mediating repulsive effects of netrin. Via this receptor transition, the same ligand can attract immature OSN axons and inhibit growth of mature OSN axons.

In the inner olfactory nerve layer and glomerular layer of the bulb, OSN axons expressing the same odorant receptor begin to fasciculate together as they course to their positions of coalescence into glomeruli. One proposed mechanism aiding this process is contact-mediated repulsion of Ephrins and Eph receptors (Cutforth et al., 2003; Serizawa et al., 2006). Consistently with this hypothesis, we detect enrichment of Ephrin and Eph receptor mRNAs in mature OSNs.

The signals that cause retention of OSN axons in glomeruli are as yet unknown, though synapse formation and the maturation of the OSN presumably solidify the OSN axon at its target (Kim and Greer 2000; Shetty et al., 2005). Semaphorins expressed in deeper layers of the olfactory bulb and inhibitory extracellular matrix molecules, such as chondroitin sulfate proteoglycans and tenascin C, surrounding the glomeruli (Shay et al., 2008) are likely candidates for maintaining OSN axons at glomeruli. Mature OSN axons also have relatively few branches, consistent with the ability of STMN3 and STMN4 to suppress axonal arborization (Klenoff and Greer, 1998; Baldassa et al., 2007; Cao et al., 2007; Poulain and Sobel, 2007). Our data suggest that, once they mature and form synapses, OSNs express predominantly inhibitory guidance cue receptors. These receptors might help to inhibit further axon growth, but mature OSNs express few of the necessary signaling protein partners to connect them to local cytoskeletal dynamics. Instead, we speculate that these receptors shift functions, perhaps regulating axon branching or transducing homeostatic signals that have effects both locally and in the nucleus.

REFERENCES

Abercrombie M. 1946. Estimation of nuclear population from microtome sections. Anat Rec 94:239–247.

Akins MR, Greer CA. 2006. Axon behavior in the olfactory nerve reflects the involvement of catenin-cadherin mediated adhesion. J Comp Neurol 499:979–989.

Andrews GL, Tanglao S, Farmer WT, Morin S, Brotman S, Berberoglu MA, Price H, Fernandez GC, Mastick GS, Charron F, Kidd T. 2008. Dscam guides embryonic axons by Netrin-dependent and -independent functions. Development 135:3839–3848.

Astic L, Pellier-Monnin V, Saucier D, Charrier C, Mehlen P. 2002. Expression of netrin-1 and netrin-1 receptor, DCC, in the rat olfactory nerve pathway during development and axonal regeneration. Neuroscience 109:643–656.

Au WW, Treloar HB, Greer CA. 2002. Sublaminar organization of the mouse olfactory bulb nerve layer. J Comp Neurol 446:68–80.

Baldassa S, Gnesutta N, Fascio U, Sturani E, Zippel R. 2007. SCLIP, a microtubule-destabilizing factor, interacts with RasGRF1 and inhibits

its ability to promote Rac activation and neurite outgrowth. J Biol Chem 282:2333–2345.

Barrientos T, Frank D, Kuwahara K, Bezprozvannaya S, Pipes GC, Bassel-Duby R, Richardson JA, Katus HA, Olson EN, Frey N. 2007. Two novel members of the ABLIM protein family, ABLIM-2 and -3, associate with STARS and directly bind F-actin. J Biol Chem 282:8393–8403.

Belluscio L, Gold GH, Nemes A, Axel R. 1998. Mice deficient in Golf are anosmic. Neuron 20:69–81.

Blackmore M, Letourneau PC. 2006. Changes within maturing neurons limit axonal regeneration in the developing spinal cord. J Neurobiol 66:348–360.

Bong YS, Lee HS, Carim-Todd L, Mood K, Nishanian TG, Tessarollo L, Daar IO. 2007. ephrinB1 signals from the cell surface to the nucleus by recruitment of STAT3. Proc Natl Acad Sci U S A 104:17305–17310.

Cai D, Shen Y, De Bellard M, Tang S, Filbin MT. 1999. Prior exposure to neurotrophins blocks inhibition of axonal regeneration by MAG and myelin via a cAMP-dependent mechanism. Neuron 22:89–101.

Camoletto P, Colesanti A, Ozon S, Sobel A, Fasolo A. 2001. Expression of stathmin and SCG10 proteins in the olfactory neurogenesis during development and after lesion in the adulthood. Brain Res Bull 54:19–28.

Cao L, Dhilla A, Mukai J, Blazeski R, Lodovichi C, Mason CA, Gogos JA. 2007. Genetic modulation of BDNF signaling affects the outcome of axonal competition in vivo. Curr Biol 17:911–921.

Chalasani SH, Sabelko KA, Sunshine MJ, Littman DR, Raper JA. 2003. A chemokine, SDF-1, reduces the effectiveness of multiple axonal repellents and is required for normal axon pathfinding. J Neurosci 23:1360–1371.

Chalasani SH, Sabol A, Xu H, Gyda MA, Rasband K, Granato M, Chien CB, Raper JA. 2007. Stromal cell-derived factor-1 antagonizes slit/robo signaling in vivo. J Neurosci 27:973–980.

Chesler AT, Zou D-J, Le Pichon CE, Peterlin ZA, Matthews GA, Pei X, Miller MC, Firestein S. 2007. A G protein/cAMP signal cascade is required for axonal convergence into olfactory glomeruli. Proc Natl Acad Sci U S A 104:1039–1044.

Cho JH, Lepine M, Andrews W, Parnavelas J, Cloutier JF. 2007. Requirement for Slit-1 and Robo-2 in zonal segregation of olfactory sensory neuron axons in the main olfactory bulb. J Neurosci 27:9094–9204.

Cloutier J-F, Ginger RJ, Koentges G, Dulac C, Kolodkin AL, Ginty DD. 2002. Neuropilin-2 mediates axonal fasciculation, zonal segregation but not axonal convergence, of primary accessory olfactory neurons. Neuron 33:877–892.

Cloutier JF, Sahay A, Chang EC, Tessier-Lavigne M, Dulac C, Kolodkin AL, Ginty DD. 2004. Differential requirements for semaphorin 3F and Slit-1 in axonal targeting, fasciculation, and segregation of olfactory sensory neurons. J Neurosci 24:9087–9096.

Col JA, Matsuo T, Storm DR, Rodriguez I. 2007. Adenylyl cyclase-dependent axonal targeting in the olfactory system. Development 134:2481–2489.

Costanzo RM 1985. Neural regeneration and functional reconnection following olfactory nerve transection in hamster. Brain Res 361:258–266.

Cutforth T, Moring L, Mendelsohn M, Nemes A, Shah NM, Kim MM, Frisen J, Axel R. 2003. Axonal Ephrin-As and odorant receptors: coordinate determination of the olfactory sensory map. Cell 114:311–322.

Doucette R. 1989. Development of the nerve fiber layer in the olfactory bulb of mouse embryos. J Comp Neurol 285:514–527.

Doucette R. 1990. Glial influences on axonal growth in the primary olfactory system. Glia 3:433–449.

Dudanova I, Tabuchi K, Rohlmann A, Sudhof TC, Missler M. 2007. Deletion of α-neuroexins does not cause a major impairment of axonal pathfinding or synapse formation. J Comp Neurol 502:261–274.

Feinstein P, Mombaerts P. 2004. A contextual model for axonal sorting into glomeruli in the mouse olfactory system. Cell 117:817–831.

Feinstein P, Bozza T, Rodriquez I, Vassalli A, Mombaerts P. 2004. Axon guidance of mouse olfactory sensory neurons by odorant receptors and the β2 adrenergic receptor. Cell 117:833–846.

Geraldo S, Khanzada UK, Parsons M, Chilton JK, Gordon-Weeks PR. 2008. Targeting of the F-actin-binding protein drebrin by the microtubule plus-tip protein EB3 is required for neuritogenesis. Nat Cell Biol 10:1181–1189.

Gitai Z, Yu TW, Lundquist EA, Tessier-Lavigne M, Bargmann CI. 2003. The netrin receptor UNC-40/DCC stimulates axon attraction and outgrowth through enabled and, in parallel, Rac and UNC-115/AbLIM. Neuron 37:53–65.

Gong Q, Shipley MT. 1996. Expression of extracellular matrix molecules and cell surface molecules in the olfactory nerve pathway during early development. J Comp Neurol 366:1–14.

Grenningloh G, Soehrman S, Bondallaz P, Ruchti E, Cadas H. 2004. Role of the microtubule destabilizing proteins SCG10 and stathmin in neuronal growth. J Neurobiol 58:60–69.

Hasegawa S, Hamada S, Kumode Y, Esumi S, Katori S, Fukuda E, Uchiyama Y, Hirabayashi T, Mombaerts P, Yagi T. 2008. The protocadherin-alpha family is involved in axonal coalescence of olfactory sensory neurons into glomeruli of the olfactory bulb in mouse. Mol Cell Neurosci 38:66–79.

Holm S. 1979. A simple sequentially rejective multiple test procedure. Scand J Statist 6:65–70.

Imai T, Sakano H. 2008. Odorant receptor-mediated signaling in the mouse. Curr Opin Neurobiol 18:251–260.

Imai T, Suzuki M, Sakano H. 2006. Odorant receptor-derived cAMP signals direct axonal targeting. Science 314:657–661.

Ishikawa R, Hayashi K, Shirao T, Xue Y, Takagi T, Sasaki Y, Kohama K. 1994. Drebrin, a development-associated brain protein from rat embryo, causes the dissociation of tropomyosin from actin filaments. J Biol Chem 269:29928–29933.

Kaneko-Goto T, Yoshihara S, Miyazaki H, Yoshihara Y. 2008. BIG-2 mediates olfactory axon convergence to target glomeruli. Neuron 57:834–846.

Kee N, Sivalingam S, Boonstra R, Wojtowicz JM. 2002. The utility of Ki-67 and BrdU as proliferative markers of adult neurogenesis. J Neurosci Methods 115:97–105.

Kim H, Greer CA. 2000. The emergence of compartmental organization in olfactory bulb glomeruli during postnatal development. J Comp Neurol 422:297–311.

Klenoff JR, Greer CA. 1998. Postnatal development of olfactory receptor cell axonal arbors. J Comp Neurol 390:256–267.

Kobayakawa K, Kobayakawa R, Matsumoto H, Oka Y, Imai T, Ikawa M, Okabe M, Ikeda T, Itohara S, Kikusui T, Mori K, Sakano H. 2007. Innate versus learned odour processing in the mouse olfactory bulb. Nature 450:503–508.

Li D, Field PM, Raisman G. 1995. Failure of axon regeneration in postnatal rat entorhinohippocampal slice coculture is due to maturation of the axon, not that of the pathway or target. Eur J Neurosci 7:1164–1171.

Lieberam I, Agalliu D, Nagasawa T, Ericson J, Jessell TM. 2005. A Cxcl12-CXCR4 chemokine signaling pathway defines the initial trajectory of mammalian motor axons. Neuron 47:667–679.

Lin D, Wang F, Lowe G, Gold GH, Axel R, Ngai J, Brunet L. 2000. Formation of precise connections in the olfactory bulb occurs in absence of odorant-evoked neuronal activity. Neuron 26:69–80.

Lundquist EA, Herman RK, Shaw JE, Bargmann CI. 1998. UNC-115, a conserved protein with predicted LIM and actin-binding domains, mediates axon guidance in C. elegans. Neuron 21:385–392.

Ly A, Nikolaev A, Suresh G, Zheng Y, Tessier-Lavigne M, Stein E. 2008. DSCAM is a netrin receptor that collaborates with DCC in mediating turning responses to netrin-1. Cell 133:1241–1254.

Mombaerts P. 2006. Axonal wiring in the mouse olfactory system. Annu Rev Cell Dev Biol 22:713–737.

Mombaerts P, Wang F, Dulac C, Chao SK, Nemes A, Mendelsohn M, Edmondson J, Axel R. 1996. Visualizing an olfactory sensory map. Cell 87:675–686.

Montag-Sallaz M, Schachner M, Montag D. 2002. Misguided axonal projections, neural cell adhesion molecule 180 mRNA upregulation, and altered behavior in mice deficient for the close homolog of L1. Mol Cell Biol 22:7967–7981.

Monti Graziadei GA. 1983. Experimental studies on the olfactory marker protein. III. The olfactory marker protein in the olfactory neuroepithelium lacking connections with the forebrain. Brain Res 262:303–308.

Monti Graziadei GA, Graziadei PP. 1979. Neurogenesis and neuron regeneration in the olfactory system of mammals. II. Degeneration and reconstitution of the olfactory sensory neurons after axotomy. J Neurocytol 8:197–213.

Morii H, Shiraishi-Yamaguchi Y, Mori N. 2006. SCG10, a microtubule destabilizing factor, stimulates the neurite outgrowth by modulating microtubule dynamics in rat hippocampal primary cultured neurons. J Neurobiol 66:1101–1114.

Miyasaka N, Knaut H, Yoshihara Y. 2007. Cxcl12/Cxcr4 chemokine signaling is required for placode assembly and sensory axon pathfinding in the zebrafish olfactory system. Development 134:2459–2468.

Nishiumi F, Komiya T, Ikenishi K. 2005. The mode and molecular mechanisms of the migration of presumptive PGC in the endoderm cell mass of *Xenopus* embryos. Dev Growth Differ 47:37–48.

Norlin EM, Alenius M, Gussing F, Hägglund M, Vedin V, Bohm S. 2001. Evidence for gradients of gene expression correlating with zonal topography of the olfactory sensory map. Mol Cell Neurosci 18:283–295.

Ozon S, Maucuer A, Sobel A. 1997. The stathmin family—molecular and biological characterization of novel mammalian proteins expressed in the nervous system. Eur J Biochem 248:794–806.

Ozon S, Mestikawy SE, Sobel A. 1999. Differential, regional, and cellular expression of the stathmin family transcripts in the adult rat brain. J Neurosci Res 56:553–564.

Pellier-Monnin V, Astic L, Bichet S, Riederer BM, Grenningloh G. 2001. Expression of SCG10 and stathmin proteins in the rat olfactory system during development and axonal regeneration. J Comp Neurol 433:239–254.

Pinching AJ, Powell TPS. 1971. The neuropil of the glomeruli of the olfactory bulb. J Cell Sci 9:347–377.

Poulain FE, Sobel A. 2007. The ''SCG10-Like Protein'' SCLIP is a novel regulator of axonal branching in hippocampal neurons, unlike SCG10. Mol Cell Neurosci 34:137–146.

Ressler KJ, Sullivan SL, Buck LB. 1994. Information coding in the olfactory system: evidence for a stereotyped and highly organized epitope map in the olfactory bulb. Cell 79:1245–1255.

Rhee J, Buchan T, Zukerberg L, Lillien J, Balsamo J. 2007. Cables links Robo-bound Abl kinase to N-cadherin-bound beta-catenin to mediate Slit-induced modulation of adhesion and transcription. Nat Cell Biol 9:883–892.

Roof DJ, Hayes A, Adamian M, Chishti AH, Li T. 1997. Molecular characterization of abLIM, a novel actin-binding and double zinc finger protein. J Cell Biol 138:575–588.

Royet JP, Souchier C, Jourdan F, Ploye H. 1988. Mophometric study of the glomerular population in the mouse olfactory bulb: numerical density and size distribution along the rostrocaudal axis. J Comp Neurol 270:559–568.

Sammeta N, Yu TT, Bose SC, McClintock TS. 2007. Mouse olfactory sensory neurons express 10,000 genes. J Comp Neurol 502:1138–1156.

Schaefer ML, Finger TE, Restrepo D. 2001. Variability of position of the P2 glomerulus within a map of the mouse olfactory bulb. J Comp Neurol 436:351–362.

Schwarting GA, Kostek C, Ahmad N, Dibble C, Pays L, Puschel AW. 2000. Semaphorin 3A is required for guidance of olfactory axons in mice. J Neurosci 20:7691–7697.

Schwarting GA, Raitcheva D, Crandall JE, Burkardt C, Puschel AW. 2004. Semaphorin 3A mediated axon guidance regulates convergence and targeting of P2 odorant receptor axons. Eur J Neurosci 19:1800–1810.

Schwob JE. 2002. Neural regeneration and the peripheral olfactory system. Anat Rec 269:33–49.

Serizawa S, Miyamichi K, Takeuchi H, Yamagishi Y, Suzuki M, Sakano H. 2006. A neuronal identity code for the odorant receptor-specific and activity-dependent axon sorting. Cell 127:1057–1069.

Shay EL, Greer CA, Treloar HB. 2008. Dynamic expression patterns of ECM molecules in the developing mouse olfactory pathway. Dev Dyn 237:1837–1850.

Shelly M, Lim BK, Cancedda L, Heilshorn SC, Gao H, Poo MM. 2010. Local and long-range reciprocal regulation of cAMP and cGMP in axon/dendrite formation. Science 327:547–552.

Shetty RS, Bose SC, Nickell MD, McIntyre JC, Hardin DH, Harris AM, McClintock TS. 2005. Transcriptional changes during neuronal death and replacement in the olfactory epithelium. Mol Cell Neurosci 30:583–600.

Shirao T, Kojima N, Obata K. 1992. Cloning of drebrin A and induction of neurite-like processes in drebrin-transfected cells. Neuroreport 3:109–112.

Skene JH, Willard M. 1981a. Axonally transported proteins associated with axon growth in rabbit central and peripheral nervous systems. J Cell Biol 89:96–103.

Skene JH, Willard M. 1981b. Characteristics of growth-associated polypeptides in regenerating toad retinal ganglion cell axons. J Neurosci 1:419–426.

Smith DS, Skene JH. 1997. A transcription-dependent switch controls competence of adult neurons for distinct modes of axon growth. J Neurosci 17:646–658.

Sobel A. 1991. Stathmin: a relay phosphoprotein for multiple signal transduction? Trends Biochem Sci 16:301–305.

Song HJ, Ming GL, Poo MM. 1997. cAMP-induced switching in turning direction of nerve growth cones. Nature 388:275–279.

Soucy ER, Albeanu DF, Fantana AL, Murthy VN, Meister M. 2009. Precision and diversity in an odor map on the olfactory bulb. Nat Neurosci 12:210–220.

Strotmann J, Conzelmann S, Beck A, Feinstein P, Breer H, Mombaerts P. 2000. Local permutations in the glomerular array of the mouse olfactory bulb. J Neurosci 20:6927–6938.

Tessier-Lavigne M, Goodman CS. 1996. The molecular biology of axon guidance. Science 274:1123–1133.

Toba Y, Tiong JD, Ma Q, Way S. 2008. CXCR4/SDF-1 system modulates development of GnRH neurons and the olfactory system. Dev Neurobiol 68:487–503.

Toda M, Shirao T, Uyemura K. 1999. Suppression of an actin-binding protein, drebrin, by antisense transfection attenuates neurite outgrowth in neuroblastoma B104 cells. Brain Res Dev Brain Res 114:193–200.

Treloar H, Tomasiewicz H, Magnuson T, Key B. 1997. The central pathway of primary olfactory axons is abnormal in mice lacking the N-CAM-180 isoform. J Neurobiol 32:643–658.

Vassar R, Chao SK, Sitcheran R, Nunez JM, Vosshall LB, Axel R. 1994. Topographic organization of sensory projections to the olfactory bulb. Cell 79:981–991.

Walz A, Rodriguez I, Mombaerts P. 2002. Aberrant sensory innervation of the olfactory bulb in neuropilins-2 mutant mice. J Neurosci 22:4025–4035.

Walz A, Mombaerts P, Greer CA, Treloar HB. 2006. Disrupted compartmental organization of axons and dendrites with olfactory glomeruli of mice deficient in the olfactory cells adhesion molecule, OCAM. Mol Cell Neurosci 32:1–14.

Whitesides JG 3rd, LaMantia AS. 1996. Differential adhesion and the initial assembly of the mammalian olfactory nerve. J Comp Neurol 373:240–254.

Williams EO, Xiao Y, Sickles HM, Shafer P, Yona G, Yang JY, Lin DM. 2007. Novel subdomains of the mouse olfactory bulb defined by molecular heterogeneity in the nascent external plexiform and glomerular layers. BMC Dev Biol 7:48.

Yoshihara Y, Kawasaki M, Tamada A, Fujita H, Hayashi H, Kagamiyama H, Mori K. 1997. OCAM: a new member of the neural cell adhesion molecule family related to zone-to-zone projection of olfactory and vomeronasal axons. J Neurosci 17:5830–5842.

Yu CR, Power J, Barnea G, O'Donnell S, Brown HE, Osborne J, Axel R, Gogos JA. 2004. Spontaneous neural activity is required for the establishment and maintenance of the olfactory sensory map. Neuron 42:553–566.

Yu TT, McIntyre JC, Bose SC, Hardin D, Owen MC, McClintock TS. 2005. Differentially expressed transcripts from phenotypically identified olfactory sensory neurons. J Comp Neurol 483:251–262.

Zheng C, Feinstein P, Bozza T, Rodriguez I, Mombaerts P. 2000. Peripheral olfactory projections are differentially affected in mice deficient in a cyclic nucleotide gated channel subunit. Neuron 26:81–91.

Zimmer C, Tiveron M-C, Bodmer R, Cremer H. 2004. Dynamics of Cux2 expression suggests that an early pool of SVZ precursors is fated to become upper cortical layer neurons. Cereb Cortex 14:1408–1419.

Zou D-J, Chesler AT, Le Pichon CE, Kuznetsov A, Pei X, Hwang El, Firestein S. 2007. Absence of adenylyl cyclase 3 perturbs peripheral olfactory projections in mice. J Neurosci 27:6675–6683.